Mutation Research - Genetic Toxicology and Environmental Mutagenesis 901 (2025) 503836

Contents lists available at ScienceDirect

Mutation Research - Genetic Toxicology and Environmental Mutagenesis

journal homepage: www.elsevier.com/locate/gentox

The transgenic MutaMouse hepatocyte mutation assay *in vitro*: Mutagenicity and mutation spectra of six substances with different mutagenic mechanisms

Alina Göpfert [a,c], David M. Schuster [b,1], Claudia Rülker [c], Michael Eichenlaub [d], Bogdan Tokovenko [e], Martina Dammann [c], Dorothee Funk-Weyer [c], Naveed Honarvar [c,*], Robert Landsiedel [a,c]

[a] *Free University of Berlin, Institute of Pharmacy, Pharmacology and Toxicology, Berlin, Germany*
[b] *University of Kassel, Kassel, Germany*
[c] *BASF SE, Experimental Toxicology and Ecology, Ludwigshafen am Rhein, Germany*
[d] *BASF SE, White Biotechnology Research, Ludwigshafen am Rhein, Germany*
[e] *BASF SE, Digitalization of Research & Development, Ludwigshafen am Rhein, Germany*

ARTICLE INFO

Keywords:
MutaMouse
Primary hepatocytes
In vitro
Next-generation sequencing
Mutation spectra

ABSTRACT

Mutagenicity testing is a component of the hazard assessment of industrial chemicals, biocides, and pesticides. Mutations induced by test substances can be detected by *in vitro* and *in vivo* methods that have been adopted as OECD Test Guidelines. One of these *in vivo* methods is the Transgenic Rodent Assay (TGRA), OECD test guideline no. 488. An analogous *in vitro* TGRA has been described, but experience with this test method is limited. In this study, six *in vivo* TGRA positive mutagens were tested in the *in vitro* TGRA based on primary MutaMouse hepatocytes. In addition to the functional read-out of the lacZ reporter gene, induced mutations were analysed by next-generation sequencing (NGS). Five of the six *in vivo* TGRA positive mutagens (N-ethyl-N-nitrosourea (ENU), ethyl methanesulfonate (EMS), mitomycin C (MMC), benzo[*a*]pyrene (B[*a*]P), and azathioprine (AZA), but not cyproterone acetate) mutated the lacZ gene *in vitro*. NGS identified mutations which matched the mutagenic mechanisms described in the literature. The alkylating agent ENU induced a greater proportion of A:T to T:A transversions than did the other alkylating agent, EMS, whereas EMS increased smaller deletions (1–4 bp). G:C to T:A transversions accounted for the majority of mutations identified after treatments with MMC and B[*a*]P, both of which form monoadducts at the guanine N2 position. AZA induced mainly G:C to A:T transitions, explained by the structural similarity of one of its metabolites to guanine. An increased proportion of mid-size changes (0.3–2.5 kb) was detected only for the crosslinking mutagen MMC. The *in vitro* TGRA based on primary MutaMouse hepatocytes is a promising *in vitro* assay for the assessment of mutation induction, reflecting many aspects of the corresponding *in vivo TGRA* and allowing for mutation spectra analysis to evaluate the induced mutations.

Abbreviations: AAALAC, Association for Assessment and Accreditation of Laboratory Animal Care; AGT, O6 -Alkylguanine DNA alkyltransferase; AM, Attachment medium; AZA, Azathioprine; B[*a*]P, Benzo[*a*]pyrene; BS, Blanch solution; CPA, Cyproterone acetate; DMEM, Dulbecco's Modified Eagle's Medium – High glucose; DMF, N,N-Dimethylformamide; DMSO, Dimethyl sulfoxide; EDTA, Ethylenediamine tetraacetic acid; EGTA, Ethylene glycol tetraacetic acid; ENU, N-Ethyl-N-nitrosourea; EMS, Ethyl methanesulfonate; FITC, Fluorescein isothiocyanate; FSC, Forward scatter; HBSS, Hank's balanced salt solution; HEPES, 4–2-Hydroxyethyl-1-piperazineethanesulfonic acid; H-insulin, Human insulin; InDel, Insertion/Deletion; MEGF, Mouse epidermal growth factor; MF, Mutant frequency; MMC, Mitomycin C; NGS, Next-generation sequencing; OECD, Organization for Economic Co-operation and Development; Pen/Strep, Penicillin, 10,000 U/mL and Streptomycin, 10 mg/mL; P-Gal, Phenyl-β-D-galactopyranoside; PHs, Primary hepatocytes; RINC, Relative increase in nuclear counts; SFM, Serum-free medium; SNP, Single nucleotide polymorphism; SSC, Side Scatter; TG, Test guideline; TGRA, Transgenic Rodent Assay.

* Corresponding author.
E-mail address: naveed.honarvar@basf.com (N. Honarvar).
[1] Present address: Department of Biology, University of Ottawa, Ottawa, Canada

https://doi.org/10.1016/j.mrgentox.2024.503836
Received 4 September 2024; Received in revised form 25 November 2024; Accepted 25 November 2024
Available online 4 December 2024

1. Introduction

Detection of potential mutagens during hazard assessment of industrial chemicals, biocides, and pesticides is needed to ensure product safety. A widely used and accepted test system for the detection of mutagenic chemicals is the Transgenic Rodent Somatic and Germ Cell Gene Mutation Assay, described in Organisation for Economic Co-operation and Development (OECD) test guideline (TG) no. 488 [1–3]. The use of transgenic rodent models harbouring recoverable reporter (trans)genes enables consistent and reliable detection and quantification of mutations in mammalian somatic and germ cells *in vivo* [2]. One of the commonly used transgenic rodent models is the MutaMouse, a mouse strain carrying multiple copies of the phage shuttle vector λgt10lacZ at a single site on chromosome 3 [2,4]. After the animals have been exposed to the test substance, the organs of interest are excised, DNA is isolated, and spontaneous and substance-induced mutations in the reporter genes are scored, with an *in vitro* positive selection assay [3,5,6]. Only phages containing non-functional, mutated reporter genes can propagate and cause plaque formation [2,5]. Since these mutation-bearing phages are easily accessible, the transgenic rodent assays not only allow a functional read-out of the catalytic activity of the lacZ gene products, but also offer the opportunity to characterize the mutations by sequencing of the mutants [1,3,7]. This is not part of the standard transgenic rodent assay (TGRA) described in OECD TG no. 488, but could be useful for the exclusion of 'jackpot' events and for identification of the most frequently targeted base pairs, valuable information for developing hypotheses about the mutagenic mechanism of a test substance [1,7,8].

As a testing method in animals, the *in vivo* TGRA is a last resort for toxicological testing; adequate non-animal methods must precede this test. The existing *in vitro* mutagenicity test systems described in OECD TGs, however, use different cells, address different genes, and use read-outs different from the *in vivo* TGRA. Therefore, individual *in vitro* methods often do not predict the *in vivo* outcome [9]. With an *in vitro* mutagenicity test system of higher accuracy (better correlation with *in vivo* outcomes), unnecessary follow-up *in vivo* genotoxicity studies could be avoided and thus laboratory animals would be spared, contributing to the 3R (Replacement, Reduction, Refinement) principle of Russel and Burch [10].

Recently, Cox et al. [11,12] and Luijten et al. [13] described an *in vitro* analogue to the *in vivo* TGRA (OECD TG no. 488), with protocols based on the work of Chen et al. [14]. The experimental procedure of the *in vitro* TGRA using metabolic competent primary MutaMouse hepatocytes is identical to its *in vivo* counterpart except for the test system used (isolated primary cells vs. whole animal). Recovery of reporter genes and mutation quantitation are identical [5,12]. The consistency of *in vitro* and follow up *in vivo* study, and the use of metabolically competent cells, can contribute to the reduction of false-positive results [9,12].

In addition to functional read-outs of lacZ reporter mutations, the easily accessible phages harbouring the mutated reporter genes can be used for mutation characterization by sequencing, which allows for correction of clonal events and furthermore prevents misinterpretation of artefacts [1,7]. Mutation characterization can also be used to identify the targeted nucleotides, important information for elucidating the mutagenic mechanism of the test substance, if the *in vivo* and *in vitro* mechanisms are the same. The studies of Besaratinia et al. [15] and Beal et al. [7] have shown that next-generation sequencing (NGS) is a valuable tool for sequencing mutant phenotypes in the *in vivo* TGRA.

To compare substance-induced mutations in the *in vitro* and *in vivo* TGRA, we have developed an NGS-based method for characterizing mutations in the lacZ reporter genes of mutant plaques obtained after treatment of primary MutaMouse hepatocytes in the *in vitro* TGRA. We have implemented the *in vitro* TGRA described by Cox et al. [12] and validated it using six known mutagens (N-ethyl-N-nitrosourea (ENU), ethyl methanesulfonate (EMS), mitomycin C (MMC), benzo[*a*]pyrene (B[*a*]P), azathioprine (AZA), and cyproterone acetate (CPA)) with distinct mutagenic mechanisms. For two of these substances (ENU and B[*a*]P) the mutation spectra in the *in vivo* TGRA studies have been described [16]. Mutant plaques were assessed for size differences in the lacZ gene as well as their mutation spectrum.

2. Materials and methods

2.1. Materials

2.1.1. Reagents

Cell culture media (Dulbecco's Modified Eagle's Medium – High Glucose (DMEM), Williams Medium E), HEPES buffer, Hank's balanced salt solutions (HBSS) with and without Ca2 + , Mg2 + and 10,000 U/mL Penicillin/10 mg/mL Streptomycin (Pen/Strep) were purchased from PAN Biotech, Aidenbach, Germany. Feta calf serum was obtained from Biowest, Nuaillé, France. Reagent-grade dimethyl sulphoxide (DMSO) for substance preparations was purchased from AppliChem, Darmstadt, Germany. Additives were obtained from Sigma-Aldrich (L-proline, L-glutamine, sodium pyruvate, ethylene glycol tetraacetic acid (EGTA), ethylenediamine tetraacetic acid (EDTA), human insulin (h-insulin) and dexamethasone) or Gibco (mouse epidermal growth factor (mEGF), distributed by Thermo Fisher Scientific, Bremen, Germay). Collagen I-coated petri dishes were purchased from Corning, Inc. (New York, USA), and collagenase HA and protease BP from VitaCyte LLC (distributed by PELObiotech GmbH, Planegg, Germany). Reagents used for cell lysis, DNA isolation, flow cytometry, and phage packaging were purchased as follows: Sigma Aldrich, Darmstadt, Germany (proteinase K, IGEPAL®-CA-630, tris(hydroxymethyl)aminomethane (TRIS), trisodium citrate, sodium dodecyl sulfate (SDS), buffer-saturated phenol, chloroform: isoamyl alcohol (24:1), 2 % (w/v) gelatin solution, 100 mg/mL ampicillin, kanamycin sulfate, N,N-dimethylformamide (DMF), yeast extract, tryptone, maltose monohydrate), Honeywell Fluka™, Seelze, Germany (sucrose, sodium chloride (NaCl), ethanol, magnesium sulfate heptahydrate (MgSO4 7 H2O)), Invitrogen™, distributed by Thermo Fisher Scientific, Bremen, Germany (20 mg/mL PureLink™ Ribonuclease A, SYTOX™ Green, Cellsorting Set up Beads for Blue Lasers), Bernd Kraft, Duisburg, Germany (citric acid monohydrate), Becton Dickinson, Heidelberg, Germany (Bacto™ Agar) and VWR, Darmstadt, Germany (phenyl-b-D-galactopyranoside). Sheath Fluid and FACS Clean were obtained from BD Biosciences, Heidelberg, Germany. The Transpack packaging extract for Lambda Transgenic Shuttle Vector Recovery was purchased from Agilent Technologies, Inc, Waldbronn, Germany. Suppliers and CAS numbers of the test chemicals (> 98 % purity) are listed in Table 1.

Polymerase Chain Reaction (PCR) Master Mix was obtained from Thermo Fisher Scientific, Bremen, Germany. Primers were purchased from Biomers.net GmbH, Ulm, Germany. For sizing PCR products, DNA-12000 ReagentKit for MultiNA, DNA-2500 ReagentKit for MultiNA and Cleaning Solution-RA for MultiNA from Shimadzu (Duisburg, Germany) were used. Reagents required for library preparation and sequencing came from Illumina, Gmbh, Berlin, Germany: Ilumina® DNA Prep Tagmentation (M) Beads, IDT for Ilumina DNA/RNA UD Indexes Set A (96 samples), Ilumina® DNA Prep_Beads + Buffers, Ilumina® DNA Prep PCR & Buffers, Ilumina® DNA Prep Sample Purification Beads, Illumina® MiniSeq™ Mid Output Reagent Cartridge 300 Cycles, Ilumina® DNA Prep Sample Purification Beads.

Table 1
CAS numbers and suppliers of the test chemicals used during the in vitro TGRA and subsequent characterization of lacZ mutations.

Compound	Supplier	CAS number
N-Ethyl-N-nitrosourea (ENU)	Sigma-Aldrich	759–53–9
Ethyl methanesulfonate (EMS)	Sigma-Aldrich	62–50–0
Mitomycin C (MMC)	Thermo Scientific	50–07–7
Benzo[*a*]pyrene (B[*a*]P)	Sigma-Aldrich	50–32–8
Azathioprine (AZA)	Sigma-Aldrich	446–86–6
Cyproterone acetate (CPA)	Sigma-Aldrich	427–51–0

2.1.2. Mice

The experiments were approved by the Landesuntersuchungsamt Rheinland-Pfalz in Koblenz, Germany (no. 23 177–07/G23–3–001). Female transgenic mice of MutaMouse strain 40.6 were purchased from Laboratory Corporation of America® Holdings (LabCorp) and kept locally under conditions approved by the Association for Assessment and Accreditation of Laboratory Animal Care (AAALAC). Mice were maintained in type II polycarbonate cages (group housing) in a specific-pathogen-free fully air-conditioned room. They were kept in a 12-hour day-night rhythm at 20–24°C and relative humidity 45–65 %. Feed (standardized pelleted feed – Granovit AG, Kaiseraugst, Switzerland) and drinking water were available ad libitum. The acclimatization period of the animals was at least 5 days. Primary hepatocytes were isolated from mice aged 12–24 weeks.

2.2. Methods

2.2.1. Isolation and culture of MutaMouse primary hepatocytes (PHs)

MutaMouse PHs were isolated and cultured according to Cox et al. [11] and Chenet al. [14] with minor adaptations to meet the local animal welfare requirements. Briefly, mice were anesthetized by an intraperitoneal application of Narcoren® (213 mg pentobarbital sodium/kg bodyweight) and exsanguinated by whole-body perfusion using blanch solution (BS; 10 mM HEPES, 1 mM EGTA, 100 U/mL penicillin–streptomycin in HBSS). After 5–6 min whole-body perfusion, a retrograde two-step collagenase liver perfusion as proposed by Seglen [17] and Cox et al. [11] was performed by accessing the vena cava inferior through the right atrium. The liver was thereby blanched for an additional 2–3 min using BS, before it was perfused with protease- and collagenase-containing perfusion medium (2000 U/mL collagenase HA and 250 U/mL BP protease in DMEM) for 15–20 min. The swollen, sponge-like liver was excised and rinsed in attachment medium (AM; 20 U/L human insulin, 4×10^{-6} mg/mL dexamethasone, 10 % FBS, and 100 U/mL penicillin-streptomycin in DMEM). To release the PHs, the liver was carefully disaggregated in AM. Dead cells and cell debris were removed by a 3 min centrifugation step at 50 *g* and 4°C and the subsequent resuspension of the pellet was in AM. Cell yield and viability were assessed (trypan blue staining) with a hemocytometer and cells were plated onto collagen-I-coated petri dishes (800,000 viable cells/100 mm or 98,000 viable cells/35 mm). After a 3 h incubation, AM was replaced with serum-free medium (SFM; 10 mM HEPES, 2 mM L-glutamine, 10 mM pyruvate, 0.35 mM L-proline, 20 U/L human insulin, 4×10^{-6} mg/mL dexamethasone, 0.01 µg/mL mEGF, and 100 U/mL penicillin–streptomycin in Williams medium E) and attached PHs were cultured overnight. Unless stated otherwise, cells were incubated at 37°C and 5 % CO_2. The next morning, cells were treated for 6 h with various concentrations of the test substances. Stock solutions of the test substances were prepared in DMSO and diluted in SFM; the final DMSO concentration was 1 %. Three technical replicates were performed for each of the tested concentrations. Following treatment, the medium was replaced with SFM and the cells were incubated for an additional 72 h.

2.2.2. Mutant frequency assessment

2.2.2.1. DNA isolation. Following the 72-h expression period, cells were lysed by replacing SFM in the 100 mm dishes with lysis buffer (10 mM Tris pH 7.6, 10 mM EDTA, 150 mM NaCl, 1 % SDS, and 1 mg/mL proteinase K; 3 mL) followed by overnight incubation at 37°C. DNA was isolated from the lysates using the phenol:chloroform extraction protocol of Cox et al. [12]. Briefly, a phenol:chloroform (1:1) purification was followed by a chloroform:isoamyl alcohol (24:1) purification containing 200 mM NaCl and a chloroform:isoamyl alcohol (24:1) purification. DNA was then precipitated using ethanol. Strings of DNA were spooled using heat-sealed glass Pasteur pipettes, washed using 70 % ethanol, air-dried, and dissolved in appropriate volumes (50–100 µL) of TEbuffer (10 mM Tris pH 7.6 and 0.1 mM EDTA).

2.2.2.2. Mutant detection. For mutant detection, the phenyl-β-D-galactopyranoside (P-Gal) positive selection method [5,12] was used. In brief, viable lambda phages carrying mutated or non-mutated lacZ reporter genes were assembled from the isolated DNA using the Transpack Packaging Extract for Lambda Transgenic Shuttle Vector Recovery. The lacZ gene construct was transferred to *E. coli* C ΔlacZ, ΔgalE, ΔrecA, Kan^r, pAA119 host cells via infection with the generated phages. Infected host cells were plated with or without P-Gal and incubated overnight at 37°C. Plaques formed under selective and non-selective conditions were counted manually. The mutant frequency (MF) was determined as the ratio of the numbers of plaques formed under selective and non-selective conditions (1 and 2):

$$1)\ \text{Total number of plaques} = \frac{\textit{number of plaques}_{\textit{non-selective conditions}} * 2485\mu L}{15\mu L}$$

$$2)\ \text{Mutant Frequency} = \frac{\text{number of mutant plaques}_{\text{selective conditions}}}{\textit{Total number of plaques}}.$$

2.2.3. Cytotoxicity

As proposed by Coxet al. [11,12], the measure of cytotoxicity used in this *in vitro* TGRA was the relative increase in nuclear counts (RINC). Briefly, cell lysis was initiated after the 72-h incubation by replacing SFM in 35 mm plates with lysis buffer I (0.584 mg/mL NaCl, 1 mg/mL sodium citrate, 0.5 µL/mL IGEPAL, 0.7 U/mL RNase A, and 0.5 µM SYTOX® green nucleic acid stain, 0.5 mL). Cells were lysed under agitation (100 rpm) in the dark at 37°C for 1 h. Lysis buffer II (85.6 mg/mL sucrose, 15 mg/mL citric acid, and 0.5 µM SYTOX® green nucleic acid stain, 0.5 mL) was added to each plate and incubated for an additional 30 min. Prior to the cytotoxicity measurement via flow cytometry, lysates were diluted with an equal volume of Sheath Fluid and 6 µm fluorescently labelled polystyrene microspheres (25 µL) were added to diluted lysate (1 mL) to enable normalization of nuclei counts.

The samples were measured at a medium flow rate (60 µL/min) in the forward scatter (FSC), side scatter (SSC), and Fluorescence 1 channels (FL1, 530/30 bandpass filter) using the FACSLyric™ flow cytometer from BD Biosciences equipped with a 488 nm laser. The flow cytometer was operated, and data was acquired using the BD FACSsuite Software version 1.4.1. The nuclei were gated based on their SYTOX® green signal. Measurement was stopped after a maximum time of 480 s or once 10,000 events were detected in the nuclei gate. Nuclei counts and RINC values were calculated according to the following formulas (3 and 4):

$$3)\ \text{Nuclei count} = \frac{(\text{population}_{2N}\times 2)+(\text{population}_{4N}\times 4)+(\text{population}_{8N}\times 8)}{\text{population}_{\text{beads}}}$$

with population_{xN} = number of events in the xN population and $\text{population}_{\text{beads}}$ = number of events in the beads population.

$$4)\ \text{RINC} = \frac{\text{Nuclei count}_{\text{treated sample}}}{\text{Nuclei count}_{\text{control sample}}}.$$

According to Cox et al. [12] RINC values < 0.2 should be considered with caution.

2.2.4. Statistical analysis

Statistical evaluation was carried out using the SAS procedure GENMOD. The numbers of mutant plaques for each sample were analyzed using general linearized models. The technical replicate was set as the statistical unit. It was assumed that the number of plaques is Poisson-distributed. Hence, the log link function was used to ensure that the number predicted by the customized model was positive. The logarithmically transformed value of the total plaque forming units was used as an offset. Pearson's chi-square (SAS Option Pscale) was used to estimate the under- or over-dispersion.

A pairwise comparison of the respective dose groups with the vehicle control group was carried out using the one-sided likelihood ratio test with the hypothesis of equal mean values. Subsequently, a Bonferroni-

Holm adjustment of the p-values was made. Furthermore, a linear trend test was carried out using the assumptions given above. All tests were carried out one-sided to a significance level of 1 %.

2.2.5. Mutant plaque collection and DNA amplification using Polymerase Chain Reaction (PCR)

Mutant plaques were individually picked using a wide bored pipette tip from test substance cultures with the highest number of mutants and transferred into individual microtubes containing SM-buffer (5.8 g/L NaCl, 2 g/L $MgSO_4 \cdot 7\ H_2O$, 0.05 M Tris-HCl, 0.01 % gelatin; 30 μL). For the vehicle control cultures, all mutant plaques were collected. As proposed by Besaratinia et al. [15] and Beal et al. [7], the isolated plaques were inactivated by boiling for 5 min. Cell debris was removed by centrifugation at 17,000 g for 5 min. Each supernatant was immediately transferred into a new microtube.

Each mutant phenotype of the lacZ reporter gene was individually amplified in two independent polymerase chain reactions (PCRs). For each reaction, a sample of the supernatant (10 μL) was mixed with PCR Master mix, 40 μL, containing 0.5 μM of each primer

(forward: 5′- GGCTTTACACTTTATGCTTC −3′, reverse: 5′- ACATAATGGATTTCCTTACG −3′ [7]), 1 ×Thermo Scientific Phire Hot Start II PCR Master mix, each nucleotide, 200 μM, and 1.5 mM $MgCl_2$. Primer sequences and amplification conditions were taken from Beal et al. [7]: initial denaturation, 95°C, 3 min, followed by 30 cycles of amplification (45 s denaturation at 95°C, 1 min primer annealing at 50°C and 4 min elongation at 72°C). The 30 cycles of amplification were followed by a final elongation period of 7 min at 72°C.

2.2.6. Preparation of pools

True mutants were identified by identical amplicon sizes of the individual replicates. Amplicon sizes were determined using the Shimadzu microchip electrophoresis system for DNA/RNA analysis MCE™- 202 MultiNA. Amplicons of true mutants were individually purified using Amicon® Ultra-0.5 centrifugal filter units according to the manufacturer's manual. The amount of DNA contained in each purified PCR product was quantified using the 1 × dsDNA HS Assay kit and the Qubit 4 Fluorometer from Invitrogen™ by ThermoFisher Scientific.

From each replicate set of purified PCR products, a separate pool was prepared using up to 100 mutant plaques for each test substance. For vehicle control samples all mutant plaques were used. Pools were prepared using an input of DNA (50 ng) from each purified mutant lacZ amplicon.

2.2.7. Next-generation sequencing using the Illumina MiniSeq

Sequencing of lacZ mutants was performed using "Sequencing by Synthesis" technology on the Illumina MiniSeq platform (Illumina, Inc.). Libraries were prepared from mutant lacZ amplicon pools using the Illumina DNA Prep kit according to the manufacture's manual (Illumina DNA Prep Checklist [18]). Libraries were quantified using the 1 × dsDNA HS Assay kit and the Qubit 4 Fluorometer from Invitrogen by ThermoFisher Scientific and qualified using the Shimadzu microchip electrophoresis system for DNA/RNA analysis MCE™-202 MultiNA with the MultiNA Smear Analysis 1.0.0.1. software.

Each library was normalized to 2 nM using Illumina Resuspension buffer. Normalized libraries were pooled and subsequently denatured by adding an equal volume of 0.1 N sodium hydroxide solution and incubating the mixture for 5 min at room temperature. Denaturation was ended by adding the same volume of 200 nM Tris-HCl. The denatured pool of libraries was diluted to a final concentration of 1.6 pM using cooled hybridization buffer, and afterwards, sequenced using the Illumina MiniSeq Mid Output Reagent Cartridge 300 cycle-kit in a 2 × 150 bp paired-end run on the Illumina MiniSeq system.

2.2.8. Bioinformatics

Bioinformatic analysis was performed according to Beal et al. [7], with a few changes based on the technological differences between the Ion Torrent and Illumina sequencing technologies. Briefly, any sequencing adapter leftovers and lower-quality bases were removed with Trimmomatic v0.38. Paired-end read mapping was done with bowtie2 v2.3.4.3, utilizing both paired and good-unpaired reads from the Trimmomatic pre-processing step and then saved to a BAM file using samtools v1.8. Next, pile-ups of all the reads per PCR replica were generated using samtools and both up- and down-stream flanks were trimmed away, so that pileups only contained the lacZ coding sequence. Per-position nucleotide frequency and indel statistics were then collected from pileups. Only nucleotide frequencies above 1 in 100 were included. This decision was based on two independent arguments:

- Illumina sequencing error rate has been reported to be 2–4 × 10^{-3} on average for R1 and R2 reads but can spike up to 1.74 × 10^{-2} for more error-prone nucleotides [19]. Thus, 1 × 10^{-2} is a slightly conservative filter to remove sequencing errors from this study's data.
- Each pool used for library preparation contained purified amplicons of at most 100 mutant plaques per sample. In the downstream analysis, mutation frequencies were hard-filtered by 1/number of plaques.

For single nucleotide polymorphism (SNP) and insertion/deletion (InDel) analysis, mutation event frequencies were collected, and filtered according to the number of plaques used for the respective sample (mutation frequency ≥ 1/number of plaques × adjustment factor (= 0.95)). For each observed mutation (defined as a combination of position along lacZ and the actual nucleotides changed), it was checked if the mutation occurred across the two PCR replicates. Mutations passing this filter were summarized and used to calculate final transition/transversion/indel rates per position.

3. Results

3.1. Validation of the in vitro TGRA for six mutagens

Experiments were performed to validate the implemented *in vitro* Transgenic Rodent Assay based on primary MutaMouse hepatocytes as described by Cox et al. [12]. During these experiments, three direct acting mutagens (ENU, EMS and MMC) and three promutagens (B[*a*]P, AZA and CPA) were tested. To evaluate the significance of substance-induced increases in MF, the MF values of treated cultures were compared to the MF values of concurrently run vehicle controls.

In the laboratory's historical control data, the vehicle control (1 % DMSO) samples showed a mean MF of 12.6 × 10^{-5} (range: 7.9–21.8 × 10^{-5}, N = 10, s.d. = 4.2 × 10^{-5}). For negative control (SFM) samples, the mean MF was 13.6 × 10^{-5} (range: 10.5–19.1 × 10^{-5}, N = 9, s.d. 2.8 × 10^{-5}). Each vehicle/negative control value was the mean of three individual cultures from individual hepatocyte preparations. Each hepatocyte preparation was derived from pooling hepatocytes from two or three animals. For the generation of the historical control data, three animal deliveries were required.

Cytotoxicity was concurrently measured by RINC. All test substances induced cytotoxicity with increasing test concentrations. Test concentrations with a high cytotoxicity (RINC <0.2) were excluded from MF assessment. These were the highest test concentration (10 μg/mL) of MMC, the two highest test concentration (5 and 10 μg/mL) of B[*a*]P, the two highest test concentration (150 and 300 μg/mL) of AZA, and the three highest test concentration (75, 150, and 300 μg/mL) of CPA.

Five of the six mutagens with distinctive mutagenic mechanisms (the direct-acting mutagens, ENU, EMS, MMC and the S9-dependent mutagens AZA and B[*a*]P, but not CPA) induced an increase in MF for at least one evaluable test concentration (Fig. 1). In addition, the three direct acting mutagens (ENU, EMS and MMC) and the promutagen B[*a*]P showed a concentration-dependent increase in MF. AZA also induced a concentration-dependent increase in MF. The induced MF at the highest

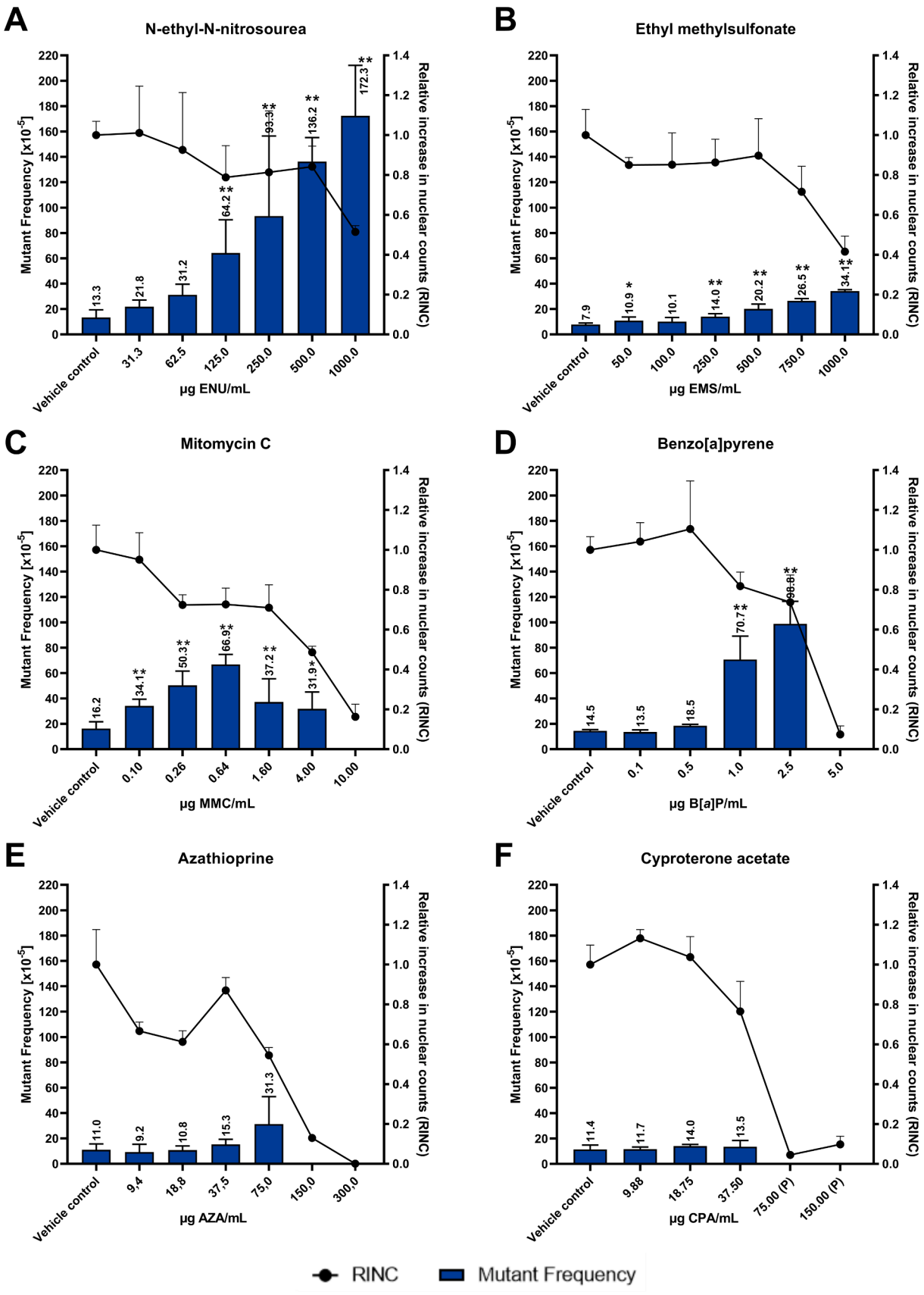

Fig. 1. Mean lacZ MF in primary MutaMouse hepatocytes induced by the mutagens ENU (A), EMS (B), MMC (C), B[*a*]P (D), AZA (E), and CPA (F). Blue bars represent mean MF (+ SD, N = 3) of the mutagens. A significant increase in MF above concurrent vehicle control is indicated by asterisks (*p < 0.05; **p < 0.01). The induced cytotoxicity at each concentration, measured as relative increase in nuclear counts, is represented as mean RINC (+ SD, N = 3) by the black crosses linked by a black line. Test groups falling <RINC = 0.2 were excluded from MF assessment to avoid confounding effects.

evaluable test concentration was not significant, but > the 95 % upper control limit of the laboratory's historical vehicle control values.

The alkylating mutagen ENU yielded a 13.0-fold increase in MF above concurrent vehicle control at the highest test concentration (1 mg/mL), the highest increase in MF observed in this study. Of the six concentrations tested, a significant increase in MF was observed for the four highest test concentrations (125, 250, and 500 μg/mL and 1 mg/mL). The other alkylating agent, EMS, induced an increase in MF above concurrent control at the four highest test concentrations of (250, 500, and 750 μg/mL and 1 mg/mL), with maximum increase = 4.3-fold at 1 mg/mL. For both test substances, the cytotoxicity (measured by RINC) increased with higher test concentrations to maxima = 0.514 and 0.415 for ENU and EMS, respectively.

The crosslinking mutagen MMC induced mutations throughout the five evaluable test concentrations (0.1024, 0.256, 0.64, 1.6, and 4.0 μg/mL). The maximum increase in MF (4.2-fold) above the concurrent vehicle control, was observed after treatment with 0.64 μg MMC/mL. At 1.6 μg MMC/mL, MF decreased and remained constant at higher concentration. Cytotoxicity (measured as decrease of nuclei relative to control, RINC) increased with the test concentration: 0.486 after treatment with 4.0 μg MMC/mL and 0.157 after treatment with 10.0 μg/mL.

The promutagen B[*a*]P induced a concentration-dependent increase in MF above concurrent vehicle control. The increases in MF were statistically significant at the two highest evaluable test concentrations (1.0 and 2.5 μg/mL). The highest increase in MF was observed at 2.5 μg B[*a*]P/mL, with a 6.8-fold increase above the concurrent control.

A concentration-dependent increase in MF was also observed after primary MutaMouse hepatocytes were exposed to AZA. The maximum increase in MF above concurrent vehicle controls was 2.8-fold. It was detected at the highest evaluable test concentration of 75.0 μg AZA/mL. However, the increase in MF was not statistically significant.

CPA did not show a significant increase in MF for any of the evaluable test concentrations, nor did it show a concentration-dependent increase in MF.

3.2. Characterization of lacZ mutations

3.2.1. Size evaluation

Mutations in the lacZ reporter gene induced by the five mutagens ENU, EMS, MMC, B[*a*]P, and AZA were characterized. Mutant lacZ phenotypes were individually amplified by PCR and the sizes of amplicons were analyzed using microchip electrophoresis. Based on the amplicon size (3222 bp) and the inherent inaccuracy (± 10 %) of the Shimadzu MultiNA (MCE-202) microchip electrophoresis system, only size changes ≥ 322 bp were measurable. For vehicle control, 2 of the 120 (= 1.7 %) analyzed mutant plaques exhibited size changes > 322 bp (Fig. 2). Treatment with MMC showed a larger proportion (27.6 %) of mutants with size changes in the range of 322–2500 bp (subsequently referred to as 'mid-size changes'). The proportions of mutants with mid-size changes induced by 1000 μg ENU/mL, 750 μg EMS/mL, 2.5 μg B[*a*]P/mL, and 75 μg AZA/mL ranged from 1.2 % to 4.8 % (Fig. 2).

3.2.2. Sequencing of mutants

For comparison, the lacZ regions from liver and ear tissues of five

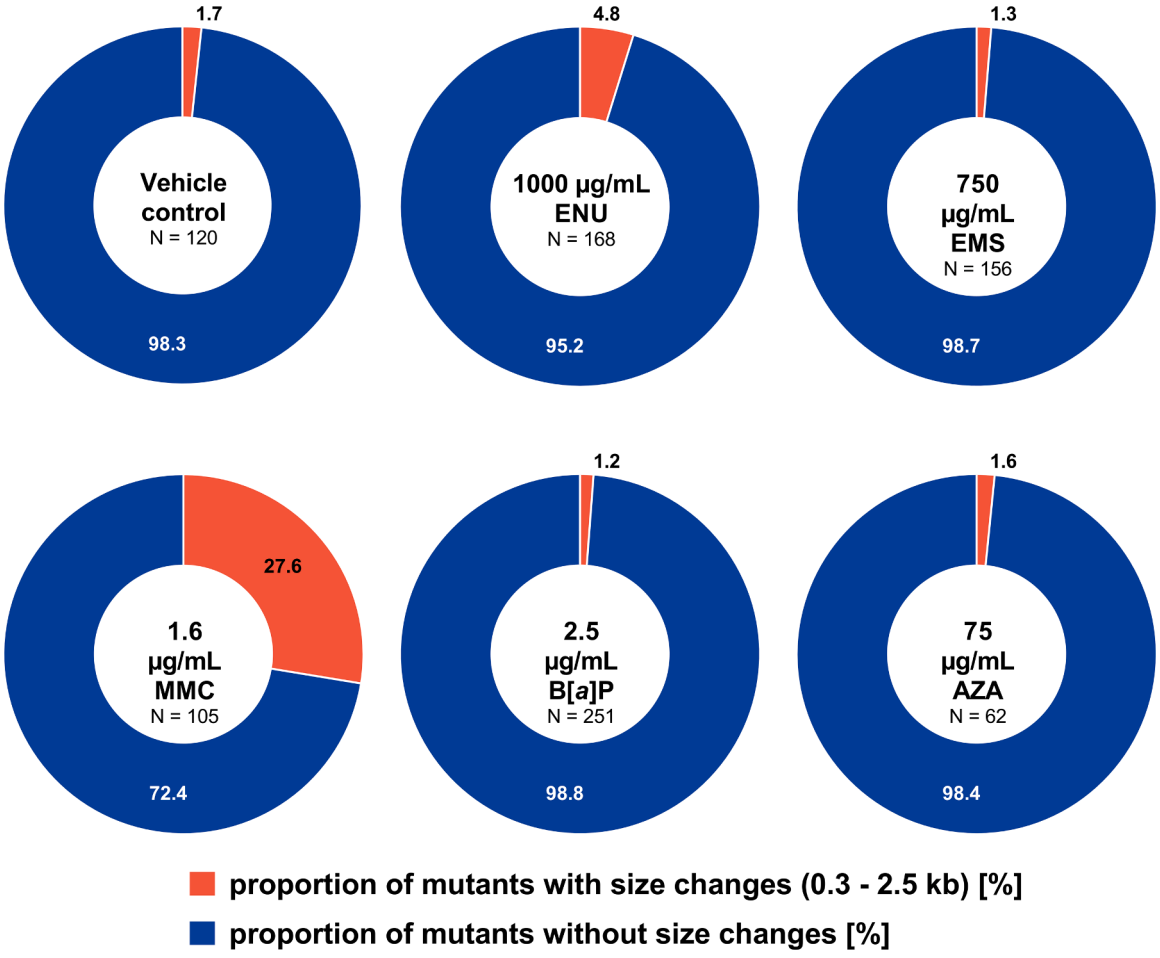

Fig. 2. Induced size changes in primary MutaMouse hepatocytes exposed to 1 % DMSO (vehicle control), 1000 μg ENU /mL, 750 μg EMS /mL, 1.6 μg MMC /mL, 2.5 μg B[*a*]P/mL and 75 μg AZA/mL. The proportion of lacZ mutants without larger size changes (322 bp – 2.5 kb) is represented in blue, whereas the proportion of mutants with larger size changes is shown in red. N describes the number of mutant lacZ phenotypes assessed for the respective test group.

untreated MutaMouse animals were sequenced, revealing four differences from the reference *E. coli lacZ* sequence [GenBank® accession number J01636.1]. The first difference was a 15-bp insertion between positions 25 and 26: 5´-AATTCCCGGGGATCC-3´. The three remaining variants were single nucleotide polymorphisms (SNPs) at positions 312 (A→G), 573 (T→C), and 3024 (C→A) of the reference sequence.

After the *in vitro* treatment of the MutaMouse PHs with the test substances, mutant lacZ phenotype sequences were compared to the lacZ sequence of the MutaMouse, as described above.

Sequencing of the 120 mutant plaques from the vehicle control revealed 44 independent mutations, throughout the 3222 bp lacZ amplicon. Most of these mutations were G:C→ A:T transitions (40.9 %) and G:C→T:A transversions (31.8 %). The proportions of the other transitions and transversions ranged from 4.6 % (A:T→G:C) to 9.1 % (A:T→T:A). No InDels were identified for vehicle control samples (Fig. 3).

The mutation spectra of ENU, EMS, MMC, B[*a*]P, and AZA are shown in Fig. 4.

For the alkylating agent ENU, 51 independent mutations were identified by sequencing a pool of 100 mutant lacZ phenotypes obtained after treatment with 1 mg ENU/mL. 53.0 % of the independent mutations identified were transversions, 45.0 % transitions, and 2.0 % small deletions. The predominant mutation types identified were G:C→A:T transitions (37.2 %) and A:T→T:A transversions (27.5 %).

Overall, 57 independent mutations were detected in 100 mutant plaques obtained after treatment with 1 mg/mL EMS. 22.2 % of the independent mutations were transversions, 55.5 % transitions, and 22.3 % small insertions and deletions (InDels). G:C→A:T transitions were the predominant mutation types, with the proportion of G:C→A:T transitions being higher after treatment with EMS (52.4 %) than after treatment with ENU (37.2 %). In addition, the proportion of small deletions was higher after EMS treatment. 21.1 % of the independent mutations identified after EMS treatment were small deletions, whereas, after ENU treatment, only 2.0 % of the independent mutations were small deletions.

The crosslinking mutagen MMC, induced 68 independent mutations in the 100 mutant plaques analysed. In total, 64.8 % of the independent mutations were transversions, 23.4 % were transitions and 11.8 % were small InDels. Of the 68 independent mutations detected after treatment with 1.6 µg MMC/mL, G:C→T:A transversions (55.3 %) and G:C→A:T transitions (20.1 %) were the most abundant mutation types.

41 independent mutations were identified in a pool of 100 mutant plaques obtained after MutaMouse PHs were exposed to 2.5 µg B[*a*]P/mL. Transversions accounted for 53.7 %, transitions 27.4 %, and small InDels 8.9 %. G:C→T:A transversions (35.6 %) and G:C→A:T (23.7 %) transitions were the most frequent mutation types.

Sequencing a pool of 62 AZA-induced mutant plaques revealed the presence of 30 independent mutations, of which 34.0 % were transversions, 60.9 % transitions, and 5.1 % small deletions. Treatment with 37.5 µg AZA/mL induced mainly G:C→A:T transitions (53.2 %) and G:C→T:A transversions (21.1 %).

4. Discussion

In this study, an *in vitro* method based on the use of PHs from transgenic MutaMouse animals was implemented and combined with NGS to predict *in vivo* mutagenicity. The *in vitro* mutagenicity assay based on MutaMouse PHs [12] was implemented and validated using six known *in vivo* TGRA mutagens. The substances induced mutations in the lacZ reporter gene which were characterized using PCR enrichment and Illumina NGS.

The mean spontaneous MF in PHs was 12.6×10^{-5}, comparable to that observed by Cox et al. (11.0×10^{-5}) [12]. Mutation characterization from the control samples identified G:C→A:T transitions and G:C→T:A transversions as the main mutation types occurring spontaneously. The same observation was made for bone marrow in an *in vivo* TGRA [16].

Because the transgenic lacZ genes in MutaMouse are heavily methylated, the high proportion of spontaneous G:C→A:T transitions is likely

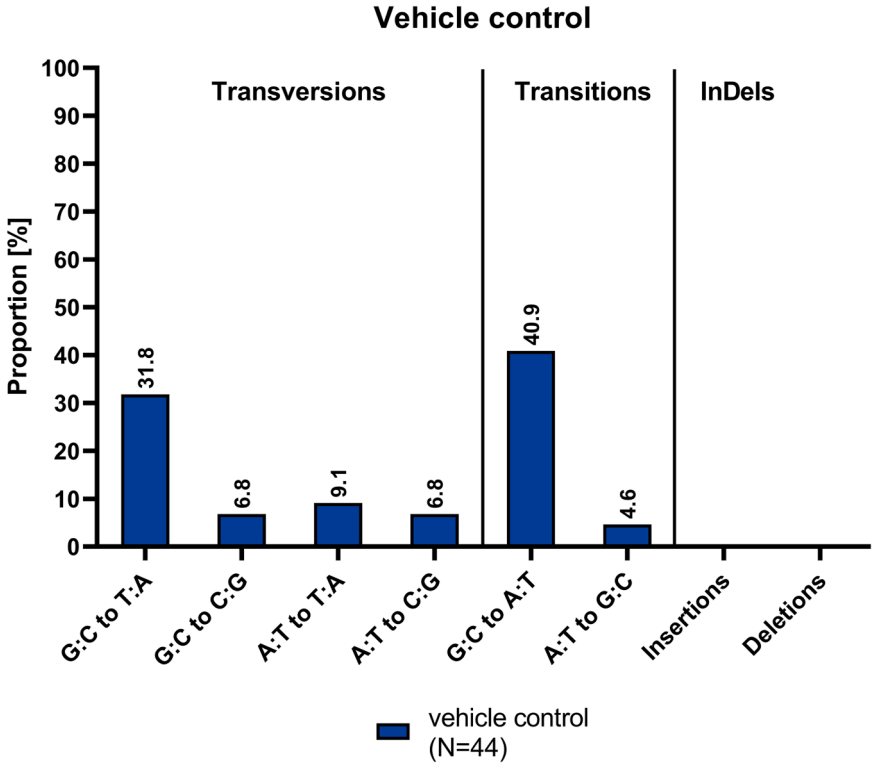

Fig. 3. LacZ mutation spectrum identified in primary MutaMouse hepatocytes exposed to 1 % DMSO (vehicle control). Blue bars represent the proportions of the particular gene mutation types indicated on the x-axis. The proportions were derived from independent mutations only. N describes the number of independent mutations identified in the pool of 120 mutant lacZ phenotypes isolated from the vehicle control samples of all experiments.

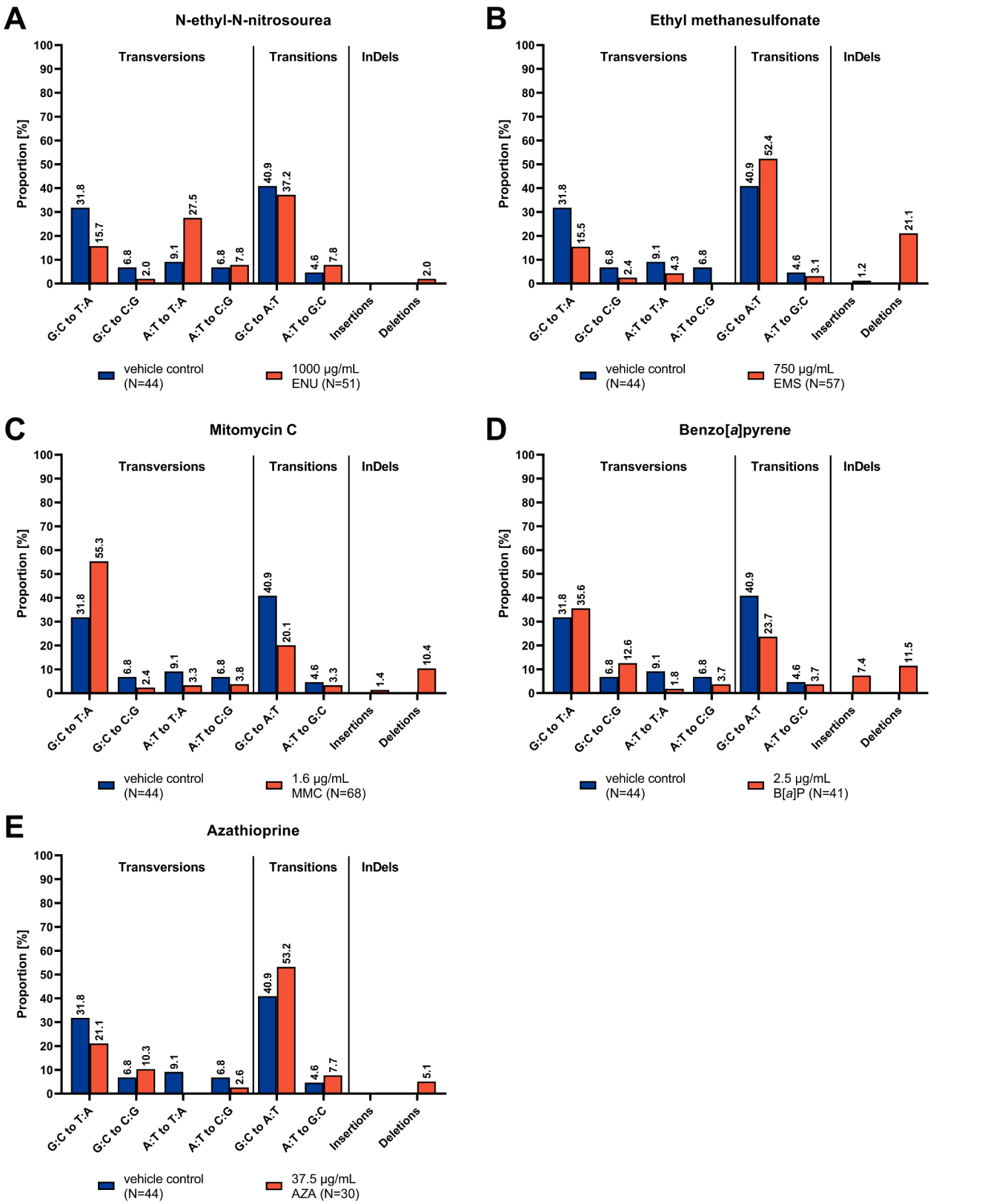

Fig. 4. Figure 4: Spontaneous (Vehicle control, 1 % DMSO) and substance-induced lacZ mutation spectra identified in primary MutaMouse hepatocytes exposed to 1000 µg ENU/mL (A), 750 µg EMS/mL (B), 1.6 µg MMC/mL (C), 2.5 µg B[*a*]P/mL (D), and 37.5 µg AZA/mL (E). The blue bars represent the mutation spectrum of vehicle controls, whereas the red bars depict the respective substance induced mutation spectrum. The height of the bars represents the proportions of the particular gene mutation types indicated on the x-axis. The proportions were derived from independent mutations only. N describes the number of independent mutations identified in the respective pools of 120 (vehicle control) or 100 (substance-induced) mutant lacZ phenotypes.

the result of deamination of methylated cytosines and subsequent mispairing [2,16,20,21]. The identified spectrum of spontaneous mutations in the *in vitro* TGRA reflected the profile observed in the *in vivo* TGRA.

Table 2 summarizes the mutagenic mechanisms of the six test substances and their responses in previously published *in vivo* and *in vitro* mutagenicity assays according to OECD TG.

The largest increase in MF was induced by the nitrosourea ENU. ENU is a direct-acting mutagen that transfers its ethyl group to nucleophilic sites in DNA, such as the O^2 or O^4 positions in T and the O^6 position in G [22,23]. The alkylated nucleotides lead to mispairing of DNA bases during cell division and consequently to mutations [22]. The mutagenic potential of ENU can also be seen in various mutagenicity assays *in vitro* (chromosomal aberration test, bacterial reverse mutation test) as well as *in vivo* (chromosomal aberration test, micronucleus test, transgenic rodent mutation assays, alkaline comet assay) [1, 24–28]. In this *in vitro* TGRA study, ENU induced a concentration-dependent increase in MF up to 13-fold increase (at 1 mg ENU/mL) above concurrent vehicle control.

ENU induced mainly G:C→A:T transitions, A:T→T:A transversions and G:C→T:A transversions. The mutation spectrum of ENU induced mutations in the *in vitro* TGRA is consistent with observations in bone marrow in the *in vivo* TGRA, Beal et al. [16]. Although a tissue-specific mutation spectrum cannot be excluded, previous error-corrected Next-Generation Sequencing data have shown that the mutation spectra of *in vivo* ENU treated Male Hsd:Sprague Dawley SD rats are similar in the bone marrow and the liver [29].

Like ENU, EMS is a direct-acting mutagen that induces mutations by alkylating nucleophilic sites of the DNA. EMS preferentially targets strong nucleophilic centres such as ring N atoms [30]. Treatment with EMS yields positive results in various mutagenicity test systems *in vitro* (bacterial reverse mutation test, chromosomal aberration test, micronucleus test, mutation test using the thymidine kinase gene) and *in vivo* (chromosomal aberration test, micronucleus test, alkaline comet assay, transgenic rodent mutation assay) [24,30]. In this study, the concentration-dependent increase in the MF observed after EMS treatment was highest (4-fold above the concurrent vehicle control) at 1 mg EMS/mL. The difference in magnitudes in the MF induced by the two alkylating agents, ENU and EMS, was likely due to differences in the alkylating mechanism and therefore the targeted nucleophiles. ENU has a high affinity for oxygen atoms, whereas EMS preferentially targets the N7 ring atom of G [31,32]. Alkylated O-atoms are no longer available for H-bond formation between DNA bases, which induces mispairing, whereas alkylation at N ring atoms is known to cause apurinic sites or chromosomal breakage [23, 31–33]. The limited sensitivity of phage based transgenic rodent systems to clastogens [2] and the inability to detect larger deletions and insertions are likely reasons for the lower MF of EMS compared to ENU.

G:C→A:T transition was the predominant mutation type identified for both alkylating agents, a mutation emerging after mispairing of O^6-alkyl-G with T [23]. The predominance of G:C→A:T transitions has often been observed in *in vitro* studies with alkylating agents. It is thought to be related to deficiency in O^6-alkylguanine DNA alkyltransferase (AGT; enzyme that removes alkyl adducts from O^6-guanine) activity of the cells (e.g., AGT- CHO) used in the *in vitro* tests [22,23]. The characterization of MutaMouse PHs, did not measure AGT activity. However, G:C→A:T transitions were also the predominant mutation type identified in bone marrow after ENU treatment of MutaMouse specimens [16].

Further predominant mutation types varied between ENU and EMS. Overall, 43.1 % of the mutations induced by ENU were A:T→T:A transversions, a mutation thought to be caused by mispairing of O^4-alkyl-T with T [22]. In contrast, only 7.5 % of the mutations induced by EMS occurred at A:T base pairs. These differences are likely the result of the higher affinity of ENU for O-atoms compared to EMS. The second predominant mutation type identified in this *in vitro* TGRA study after EMS treatment was small apurinic sites (1–4 bp deletions) which are thought to emerge after alkylation of ring N-atoms [31].

Table 2
Mutagenic mechanisms of the six mutagens tested, their test results in various in vivo and in vitro mutagenicity test systems, *and* their overall response in this in vitro TGRA.

Test substance	Mutagenic mechanism	Result		
		In vivo	***In vitro***	***In vitro* TGRA** (this study)
N-Ethyl-*N*-nitrosourea	Alkylation	+ CA [24] + MN [24] + TGRA [24]	+ *in vitro* TGRA [12] + HPRT [13] + Ames [24] + CA [24]	+
Ethyl methanesulfonate	Alkylation	+ CA [24] + MN [24] + Comet [24] + TGRA [24] + Carc [24]	+ Ames [24] + CA [24] + MLA [24] + MN [24]	+
Mitomycin C	Mono- and Bis-adduct formation (crosslinking activity)	+ CA [24] + MN [24] + TGRA [24]	+ *in vitro* TGRA [13] + Ames [24] + CA [24] + HPRT [13] + MLA [24]	+
Benzo[*a*]pyrene	Bulky DNA adduct formation after metabolic activation	+ MN [24] + UDS [24] + TGRA [24]	+ *in vitro* TGRA [12, 13] + Ames [24] + CA [24] + HPRT [13] + MLA [24]	+
Azathioprine	Nucleotide analog after metabolic activation	+ CA [24] + MN [24] + TGRA [47]	+ Ames [24] + CA [24]	+
Cyproterone acetate	DNA adduct formation after metabolic activation	+ MN [24] + UDS [24] + TGRA [53]	- Ames [24] - CA [24] - HPRT [51]	-

+ positive; - negative
CA: Mammalian Chromosome Aberration Test (*in vivo*: OECD TG no. 475; *in vitro*: OECD TG no. 473)
HPRT: *In vitro* Mammalian Cell Gene Mutation Tests using the Hprt and xprt genes (OECD TG no. 476)
MLA: Mouse Lymphoma Assay (*In vitro* Mammalian Cell Gene Mutation Tests Using the Thymidine Kinase Gene; OECD TG no. 490)
MN: Mammalian Micronucleus Test (*in vivo*: OECD TG no. 474; *in vitro*: OECD TG no. 487)
Ames: Bacterial Reverse Mutation Test (OECD TG no. 471)
TGRA: Transgenic Rodent Gene Mutation Assay (*in vivo*: OECD TG no. 488; *in vitro*: no OECD TG)
UDS: Unscheduled DNA Synthesis (UDS) Test with Mammalian Liver Cells *in vivo* (OECD TG no. 486)

Overall, the observations agree with findings from an *in vivo* TGRA study in MutaMouse performed by Suzuki et al. [34]. Not only did they observe a stronger increase in lacZ MF after treatment with ENU (compared to EMS), but they also detected differences in the mutation spectra of the two alkylating agents [34]. They identified G:C→A:T transitions as the predominant mutation type after EMS treatment *in vivo*, whereas after ENU treatment 40 % of the mutations were A:T base-pair substitutions [34].

MMC is an anticancer chemotherapeutic known to form DNA adducts at the N2-position of G after reductive activation by endogenous flavoreductases [35]. These bulky DNA adducts are expected to induce mispairing of DNA bases during DNA replication, resulting in mutations [36]. Loss of carbamate ions from monoalkylation products gives rise to a second alkylation site, which can either form inter- or intrastrand crosslinks [37].

In this study, the MF showed a bell-shaped curve over the five evaluable MMC concentrations, with maximum MF at 0.64 μg MMC/mL. Different mutation types were detected: base-pair mutations (transitions/transversions) and frameshift mutations (insertions/deletions, InDels). Characterization of MMC-induced mutations in an *in vivo* TGRA in the bone marrow of gpt delta transgenic mice revealed tandem-base substitutions and deletions in the range of 110 bp to 8 kb [36]. The decrease in MF at MMC concentrations > 0.64 μg/mL observed in this *in vitro* TGRA study is likely to be caused by an increasing number of crosslinks and the thereby related occurrence of larger InDels (i.e. clastogenic events). As the cross-linking activity of MMC is promoted by an increasing G:C content [38], a high induction of DNA-strand linkage is supposed to occur in the G:C-rich lacZ reporter gene (56 % of G:C nucleotides, [39]). It was shown in *in vivo* TGRAs, that clastogenic events are less likely to be detected when bacteriophage shuttle vector-based transgenes were used [40]. As the *in vitro* TGRA performed in this study is based on MutaMouse PHs harbouring λ phage shuttle vectors, it is supposedly less suitable to detect the increasing proportion of large InDels. However, indications for the clastogenic activity of MMC were provided during size evaluation of amplified lacZ reporter genes using microchip electrophoresis. MMC was the only test substance that increased the proportion of mutant phenotypes with size changes in the range of 0.3 – 2.5 kb (16.2-fold increase over vehicle control). Nevertheless, the use of bacteriophage transgenes was not as conclusive for the assessment of clastogenic substances as for plasmid-based transgenic rodent models as seen in previous studies.

Characterization of MMC-induced mutations identified G:C base pairs as the main target. In total, 77.8 % of MMC induced mutations occurred at G:C base pairs, with G:C→T:A transversions and G:C→A:T transitions the predominant types. These mutations were also predominantly seen after MMC treatment in the bone marrow of gpt delta mice *in vivo* and GDL1 cells (lung fibroblasts isolated from gpt delta mice) *in vitro* [36,37]. Despite the use of different tissues, the observed concordance in the mutation spectrum suggests a tissue non-specific mechanism of action for this substance, which is likely because MMC does not need to be metabolized in order to induce mutations.

With a 6.8-fold increase in MF over vehicle control, B[*a*]P induced the strongest increase in MF of the three promutagens tested. B[*a*]P, a polycyclic aromatic hydrocarbon originating from incomplete combustion of organic matter, is a known human carcinogen which forms bulky DNA adducts after metabolic activation [41–43]. In other *in vitro* mutagenicity test systems, the mutagenic potential of B[*a*]P is only seen with the addition of an exogenous activation system [12,28]. The strong increase in MF without the addition of an exogenous activation system was observed after B[*a*]P treatment of primary MutaMouse hepatocytes in this study, which compliments the studies by Cox et al., 12] and Luijten et al. [13]. Therefore, the authors recommend B[*a*]P as a suitable positive control in the *in vitro* TGRA, especially for mutagens requiring metabolic activation. The strong increase in MF after B[*a*]P treatment observed in multiple laboratories demonstrates the metabolic competence of the freshly isolated primary MutaMouse hepatocytes and also indicates the reproducibility of the *in vitro* TGRA in MutaMouse PHs. For a better evaluation of the between-laboratory reproducibility of the *in vitro* TGRA in MutaMouse PHs, benchmark concentration analysis was performed as described by Cox et al. [12] for the substances B[*a*]P and ENU (data not shown). For both substances, the BMC_{100} confidence intervals obtained in this study were overlapping with the BMC_{100} confidence intervals of Cox et al. [12]. Accordingly, there was no difference in sensitivity between the two laboratories regarding the detection of B[*a*]P and ENU-induced mutagenicity in the *in vitro* TGRA. This observation further demonstrates the inter-laboratory reproducibility of the *in vitro* TGRA in MutaMouse PHs.

In the *in vivo* TGRA studies by Beal et al. [7] and Hakura et al. [44], G:C→T:A transversions were the most frequent mutations induced by B[*a*]P. G:C base pairs were also the primary target of B[*a*]P mutagenesis in this *in vitro* TGRA study. G:C→T:A transversions, G:C→A:T transitions, and small deletions were the predominant mutation types identified. These observations match the mutagenic mechanism of B[*a*]P according to which mispairing of DNA bases occurs after bulky DNA adduct formation at the N2 position of G by one of B[*a*]P's metabolites [16,42]. The *in vivo* results described above refer to either bone marrow [7,16] or spleen and forestomach [44]. Although tissue-specific mutagenicity cannot be ruled out, it is highly likely that the mechanisms of action of B[*a*]P in the tested tissues are similar. An error-corrected NGS study [45] corroborates this, showing a very similar mutation spectrum in the liver of B[*a*]P treated MutaMice.

The promutagen AZ, is an immunosuppressant known to be carcinogenic in humans [46,47]. In this *in vitro* TGRA study, none of the AZA concentrations tested induced a statistically significant increase in MF, despite a maximally 2.8-fold increase in the MF as compared to the vehicle control. However, a concentration-dependent increase in MF was evident in addition to a maximum induced MF outside the laboratory's historical vehicle control data. These results concur with the results of an *in vivo* TGRA study in MutaMouse performed by Smith et al. [47]. 24 h after a 5-day treatment, AZA induced a 2.0-fold, statistically significant increase in MF in the liver only at the highest dose (100 mg/kg body weight/day). 25 Days after a 5-day treatment, the increase in MF was no longer statistically significant, despite a 1.3–1.5-fold increase in the MF as compared to the vehicle control. Not AZA itself, but one of its metabolites (6-thioguanine) is mutagenic because of its similarity to the DNA base G [48]. If incorporated into the DNA strand, 6-thioguanine nucleotides are non-enzymatically methylated by S-adenosylmethionine [49]. The resulting 6-methylthioguanine pairs with T rather than C, inducing G:C→A:T transitions [50]. Characterization of AZA-induced mutations from this *in vitro* TGRA study identified G:C→A:T transitions as the predominant mutation type. Since mutation induction by AZA requires not only metabolic activation but also the incorporation of the formed nucleotide analogues during DNA replication, it is likely that the 6 h exposure period was too short. AZA should be tested in the *in vitro* TGRA with longer exposure times within the time frame during which the metabolic capacity of the PHs persists (24 h [11]). Extended exposure times would be hard to achieve with exogenous activation systems such as S9 mix, but should be feasible with metabolically competent PHs.

CPA is a synthetic steroidal anti-androgen used for the treatment of prostate carcinoma and of androgenisation symptoms in women [51]. CPA induces DNA repair and forms DNA adducts in PHs from female rats [51,52]. DNA adduct formation requires metabolic reduction of a keto group and subsequent sulfonation at the hydroxy group [52]. *In vivo*, CPA induced mutations in the liver of transgenic female Big Blue™ F344 rats [53]. In this *in vitro* TGRA based on female MutaMouse PHs none of the evaluable test concentrations of CPA caused a significant increase in MF over the control. Due to severe cytotoxicity observed in MutaMouse PHs, 37.5 μg CPA/mL was the highest evaluable test concentration in this *in vitro* TGRA. *In vivo*, significant increases in MF were observed in the liver of female Big Blue™ F344 rats, when animals were exposed to a single dose of 200 mg/kg [53]. To estimate weather the discrepancies

between the *in vitro* and *in vivo* TGRA findings result from different tissue/cell exposure levels, *in vitro*-to-*in vivo* extrapolation (IVIVE) could be used to estimate the *in vivo* dose required to reach a tissue exposure level comparable to the highest evaluable *in vitro* concentration of CPA. One other explanation for the discrepancy between the obtained *in vitro* results with the *in vivo* data could be a potential lack of sulfotransferase activity in the PHs. Cox et al. [11] have considered the metabolic activity of the isolated PHs; however, their assessment was primarily focused on cytochrome P450 activities. The activities of enzymes that catalyze PH conjugations still need to be studied.

The implemented *in vitro* TGRA using MutaMouse PHs was able to identify the mutagenic potential of ENU, EMS, MMC, B[*a*]P, and AZA without the addition of an exogenous activation system (relevant for the promutagens B[*a*]P and AZA). Obviously, the PHs retain sufficient metabolic competence during the *in vitro* TGRA to activate these promutagens. Before the *in vitro* TGRA based on PHs can complement or replace available *in vitro* mammalian cell-based mutagenicity assays in the current test battery for mutagenicity assessment, further studies are required to characterize the sensitivity and specificity of the assay. Additional substances need to be tested, including substances known to give true positive, true negative, misleading positive, and false negative results in current *in vitro* mutagenicity assays. The selection and the number of the compounds to be used in the validation of the assay should rely on previously published work [54].

Further attention should be paid to cytotoxicity assessment in the *in vitro* TGRA. First, cytotoxicity is assessed in separate cultures than those used for MF evaluation. The cultures differ in size, which could lead to different culture conditions. Ideally, cytotoxicity should be assessed using the same cultures as for lacZ MF assessment. Second, the currently used threshold for cytotoxicity should be reviewed. Based on OECD test guidelines for *in vitro* mammalian cell mutation assays using the Hprt, Xprt and thymidine kinase genes, Cox et al. [12] suggested a RINC value = 0.2 as the threshold for cytotoxicity in the *in vitro* TGRA. However, there has been no research on the effect of cytotoxicity on the MF in primary MutaMouse hepatocytes. Further studies should be performed using substances that are cytotoxic but not mutagenic. Third, the cytotoxicity assessment provides no information about the proliferation capacity of the isolated cells. Since DNA replication is necessary to obtain a manifested mutation from DNA damage, proliferation capacity would be a beneficial endpoint to exclude sensitivity impairment in case of negative test results. Flow-cytometric assessment could be extended using cell linkers to quantify the percentage of proliferating cells.

Mutation spectra that were induced by ENU, EMS, MMC, and B[*a*]P in MutaMouse PHs were consistent with mutation spectra obtained in previously published *in vivo* TGRAs [7,16,36,44]. For AZA, no data on the mutation spectra in an *in vivo* TGRA study were available. Nevertheless, the identified mutation spectra in this *in vitro* TGRA study match the mutagenic mechanisms of AZA described in the literature [48,50]. These findings demonstrate that mutagenesis in the *in vitro* TGRA based on MutaMouse PHs mirrors *in vivo* TGRA mutagenesis.

The mutation characterization methods described by Beal et al. [7] and Besaratinia et al. [15] detected mutations by a functional read-out of the target gene (lacZ), and subsequent sequencing of isolated mutants. Characterization of mutations solely using (Illumina) next generation sequencing does not detect clastogenicity since this method involves DNA fragmentation during library preparation, sequence alignment and generation of consensus sequences in the end. The herein study additionally addressed clastogenicity by a preceding size integrity evaluation using microchip electrophoresis.

In order to address size changes in the transgenic reporter genes, size evaluation using microchip electrophoresis was incorporated into the mutation characterization procedure. Visual assessment of size alterations could only detect a small portion of the amplicon size. This is because of the limited resolution in the images in addition to the hampered retrieval of mutants with larger size changes when bacteriophage transgenes are used. With deletions/insertions of larger DNA fragments in the transgene, it is likely that at least one of the cos sites required for phage packaging is affected [2,40], thus impeding a successful assembly of the l phages. Accordingly, the visual evaluation hardly revealed the clastogenic activity of the test substances. When the amplicon sizing feature of the Shimadzu microchip electrophoresis device was used, deletions in the range of 0.3–2.5 kb became readily detectable. The lower limit of 0.3 kb resulted from the inherent inaccuracy of the device in size calling (± 10 % of amplicon size), whereas the upper limit of 2.5 kb was the maximum observed size change. Using technical amplicon sizing, size evaluation became more conclusive. The clastogenic activity of MMC was detected as it was the only substance that induced an increased proportion of mutant lacZ phenotypes with size changes in the range of approximately 0.3–2.5 kb. This is consistent with the previously described DNA crosslinking activity of MMC which induces DNA strand breakages [36]. However, the MMC-results were not as prominent as in the study of Luijtenet al. [13] where lacZ plasmid mice were used. These observations demonstrate the limitation of phage shuttle vector based transgenic models in contrast to plasmid based transgenic models regarding the evaluation of clastogenic mutagens.

To assess size integrity, each mutant plaque was processed individually. Accordingly, for each mutant plaque, the lacZ reporter gene was individually amplified by PCR. In previous mutation characterization studies of transgenic rodent studies pools containing multiple plaques were used as template for amplification [7,15]. Since more reactions are required for individual plaque processing, the implemented method is slightly more laborious. However, with the development towards high throughput and automated performances of PCRs, multiple samples can be processed simultaneously, making the increased workload negligible. In addition, single plaque processing avoids under- and over-representation of mutant phenotypes since pools for sequencing are prepared using equal DNA input amounts from each mutant phenotype. If pools are prepared prior to PCR, mutant phenotypes from larger plaques are likely to be overrepresented in the mixture, whereas mutant phenotypes from smaller plaques are likely to be underrepresented. In summary, both methods (single plaque processing and processing of plaque pools) seem to be well suited for characterizing occurring mutations in the *in vitro* TGRA. In this study, individual plaque processing was deemed useful for two reasons: information on the induction of size changes in the range of approximately 0.3–2.5 kb is provided (a hint for clastogenic activity) and under- or over-representation of mutant phenotypes in the pool used for sequencing is avoided.

5. Conclusions

We have combined an *in vitro* TGRA based on MutaMouse PHs with a mutation characterization procedure involving size evaluation and sequencing of mutated LacZ reporter genes to identify mutation types. For five of the six mutagens tested, the *in vitro* results coincided to the *in vivo* results described in literature. This included test substances requiring metabolic activation. Accordingly, the PHs retain sufficient metabolic competence in the *in vitro* TGRA and the functional read-out of the lacZ reporter gene products, was sufficient to recognize a mutagenic potential. Therefore, the *in vitro* TGRA based on MutaMouse PHs is suggested to be a suitable *in vitro* mutagenicity test system to predict the *in vivo* outcome. This could prevent false positive results *in vitro* and thus avoid unnecessary *in vivo* follow-up studies based on these false positive *in vitro* test results. If the correlations of *in vitro* PHs and *in vivo* results are further substantiated, a mutagenicity assay in PHs could minimize the need for *in vivo* studies altogether.

In addition, clastogenic activity of the test substances can be identified by size evaluation of the mutants and sequencing of the lacZ gene offers insight into the gene mutagenic mechanism of the test substances *in vitro*. The *in vitro* mutation spectra of ENU, EMS, MMC, B[*a*]P were in accordance with the *in vivo* TGRA outcomes. *In vivo* mutation spectra of AZA were not available, but its mutagenic potential *in vivo* was also observed *in vitro*; albeit the *in vitro* study design may need optimization

for this compound. Even more so, the current design of the *in vitro* TGRA using MutaMouse PHs was not suitable to detect the *in vivo* mutagenicity of CPA.

The agreement in mutation spectra in this *in vitro* study and published *in vivo* TGRA studies shows that analysing a total of 100 mutant plaques per test substance is sufficient. This method is suitable for routine testing since differently barcoded libraries and pools from multiple substances can be analysed in a single run at relatively low costs. Incorporating mutation characterization in an *in vitro* mutagenicity test not only reduces the number of false positive test results by correcting for mutational jackpot events, but also provides information on the mutagenic mechanism of the test substance and thus improves the hazard and risk assessment for potential candidates in early stages of development.

CRediT authorship contribution statement

Claudia Rülker: Investigation. **Michael Eichenlaub:** Writing – review & editing, Investigation, Formal analysis, Data curation. **Bogdan Tokovenko:** Investigation, Formal analysis, Data curation. **Naveed Honarvar:** Writing – original draft, Validation, Methodology, Conceptualization. **Robert Landsiedel:** Writing – review & editing, Supervision, Resources, Funding acquisition, Conceptualization. **Martina Dammann:** Formal analysis, Data curation. **Dorothee Funk-Weyer:** Writing – review & editing, Resources, Formal analysis. **Alina Göpfert:** Writing – original draft, Methodology, Investigation, Data curation. **David M. Schuster:** Investigation, Data curation.

Declaration of Competing Interest

Alina Göpfert, Claudia Rülker, Michael Eichenlaub, Bogdan Tokovenko, Martina Dammann, Dorothee Funk-Weyer, Naveed Honarvar and Robert Landsiedel are employees of BASF SE, a chemical company which may use the assay to develop and register commercial products.

Acknowledgements

The authors would like to thank Paul A. White and Julie Cox (Health Canada) for their advice on the implementation of the *in vitro* TGRA and for providing the *E. coli* C ΔlacZ, ΔgalE, ΔrecA, Kan^r, pAA119 host strain. The authors are also grateful for the advice of Katharina Belgasmi (Leibniz Research Centre for Working Environment and Human Factors) regarding the isolation of primary mouse hepatocytes. They appreciate Vanessa Hebestreit's (BASF SE) indispensable support in the isolation of primary hepatocytes. The authors also acknowledge the laboratory assistance of Natascha Partosa, Julia Henn, Bärbel E. Moos, Viola Cetto, Niels Söhnlein, Andrea Schmidt, Stefan Hermann, and Annette Wegerle (BASF SE). The authors would also like to thank Marc Beal and Matthew Meier (Health Canada) for providing the bioinformatic scripts required for analysis of sequencing data in addition to their advice in data interpretation. This work was funded by BASF Key Technology Capability Building Alternative Toxicological Methods, BASF SE, Germany.

Data Availability

Data will be made available on request.

References

[1] OECD, Test No. 488: Transgenic Rodent Somatic and Germ Cell Gene Mutation Assays, 2022.
[2] I.B. Lambert, T.M. Singer, S.E. Boucher, G.R. Douglas, Detailed review of transgenic rodent mutation assays, Mutat. Res 590 (2005) 1–280.
[3] M.J. Meier, M.A. Beal, A. Schoenrock, C.L. Yauk, F. Marchetti, Whole genome sequencing of the mutamouse model reveals strain- and colony-level variation, and genomic features of the transgene integration site, Sci. Rep. 9 (2019) 13775.
[4] P.A. White, M. Luijten, M. Mishima, J.A. Cox, J.N. Hanna, R.M. Maertens, E. P. Zwart, In vitro mammalian cell mutation assays based on transgenic reporters: a report of the International Workshop on Genotoxicity Testing (IWGT), Mutat. Res 847 (2019) 403039.
[5] J. Gingerich, L. Soper, C. Lemieux, F. Marchetti, G. Douglas, Transgenic rodent gene mutation assay in somatic tissues, in: L. Sierra, I. Gaivão (Eds.), Genotoxicity and DNA Repair. Methods in Pharmacology and Toxicology, Humana Press, New York, NY, 2014, pp. 305–321.
[6] J.M. O'Brien, M.A. Beal, J.D. Gingerich, L. Soper, G.R. Douglas, C.L. Yauk, F. Marchetti, Transgenic rodent assay for quantifying male germ cell mutant frequency, J. Vis. Exp. (2014) e51576.
[7] M.A. Beal, R. Gagné, A. Williams, F. Marchetti, C.L. Yauk, Characterizing benzo[*a*] pyrene-induced lacZ mutation spectrum in transgenic mice using next-generation sequencing, BMC Genom. 16 (2015) 812.
[8] J.A. Heddle, On clonal expansion and its effects on mutant frequencies, mutation spectra and statistics for somatic mutations in vivo, Mutagenesis 14 (1999) 257–260.
[9] D. Kirkland, S. Pfuhler, D. Tweats, M. Aardema, R. Corvi, F. Darroudi, A. Elhajouji, H. Glatt, P. Hastwell, M. Hayashi, P. Kasper, S. Kirchner, A. Lynch, D. Marzin, D. Maurici, J.R. Meunier, L. Müller, G. Nohynek, J. Parry, E. Parry, V. Thybaud, R. Tice, J. van Benthem, P. Vanparys, P. White, How to reduce false positive results when undertaking in vitro genotoxicity testing and thus avoid unnecessary follow-up animal tests: report of an ECVAM Workshop, Mutat. Res 628 (2007) 31–55.
[10] J. Tannenbaum, B.T. Bennett, Russell and Burch's 3Rs then and now: the need for clarity in definition and purpose, J. Am. Assoc. Lab Anim. Sci. 54 (2015) 120–132.
[11] J.A. Cox, E.P. Zwart, M. Luijten, P.A. White, The development and prevalidation of an in vitro mutagenicity assay based on MutaMouse primary hepatocytes, part I: isolation, structural, genetic, and biochemical characterization, Environ. Mol. Mutagen 60 (2019) 331–347.
[12] J.A. Cox, E.P. Zwart, M. Luijten, P.A. White, The development and prevalidation of an in vitro mutagenicity assay based on MutaMouse primary hepatocytes, Part II: Assay performance for the identification of mutagenic chemicals, Environ. Mol. Mutagen 60 (2019) 348–360.
[13] M. Luijten, E.P. Zwart, M.E. Dollé, M. de Pooter, J.A. Cox, P.A. White, J. van Benthem, Evaluation of the LacZ reporter assay in cryopreserved primary hepatocytes for In vitro genotoxicity testing, Environ. Mol. Mutagen 57 (2016) 643–655.
[14] G. Chen, J. Gingerich, L. Soper, G.R. Douglas, P.A. White, Induction of lacZ mutations in Muta™Mouse primary hepatocytes, Environ. Mol. Mutagen 51 (2010) 330–337.
[15] A. Besaratinia, H. Li, J.I. Yoon, A. Zheng, H. Gao, S. Tommasi, A high-throughput next-generation sequencing-based method for detecting the mutational fingerprint of carcinogens, Nucleic Acids Res 40 (2012) e116.
[16] M.A. Beal, M.J. Meier, D.P. LeBlanc, C. Maurice, J.M. O'Brien, C.L. Yauk, F. Marchetti, Chemically induced mutations in a MutaMouse reporter gene inform mechanisms underlying human cancer mutational signatures, Comm. Biol. 3 (2020) 438.
[17] P.O. Seglen, Chapter 4 Preparation of Isolated Rat Liver Cells, in: D.M. Prescott (Ed.), Methods in Cell Biology, Academic Press, 1976, pp. 29–83.
[18] I. Inc., Illumina DNA Prep Checklist, Document # 1000000033561 v05, https://support.illumina.com/content/dam/illumina-support/documents/documentation/chemistry_documentation/illumina_prep/illumina-prep-checklist-1000000033561-05.pdf, 2020.
[19] M. Schirmer, R. D'Amore, U.Z. Ijaz, N. Hall, C. Quince, Illumina error profiles: resolving fine-scale variation in metagenomic sequencing data, BMC Bioinforma. 17 (2016) 125.
[20] H. Ikehata, M. Takatsu, Y. Saito, T. Ono, Distribution of spontaneous CpG-associated G:C → A:T mutations in the lacZ gene of Muta™ mice: Effects of CpG methylation, the sequence context of CpG sites, and severity of mutations on the activity of the lacZ gene product, Environ. Mol. Mutagen 36 (2000) 301–311.
[21] R.C. Poulos, J. Olivier, J.W.H. Wong, The interaction between cytosine methylation and processes of DNA replication and repair shape the mutational landscape of cancer genomes, Nucl. Acids Res 45 (2017) 7786–7795.
[22] J.K. Noveroske, J.S. Weber, M.J. Justice, The mutagenic action of N-ethyl-N-nitrosourea in the mouse, Mamm. Genome 11 (2000) 478–483.
[23] J.P. O'Neill, DNA damage, DNA repair, cell proliferation, and DNA replication: how do gene mutations result? Proc. Natl. Acad. Sci. USA 97 (2000) 11137–11139.
[24] OECD, OECD/ENV/JM/MONO(2009)7, Series on Testing and Assessment Number 103: Detailed Review Paper on Transgenic Rodent Mutation Assays, OECD Environment, Health and Safety Publications, Paris, 2009, pp. 1–281.
[25] OECD, Test No. 475: Mammalian Bone Marrow Chromosomal Aberration Test, 2016.
[26] OECD, Test No. 474: Mammalian Erythrocyte Micronucleus Test, 2016.
[27] OECD, Test No. 489: In Vivo Mammalian Alkaline Comet Assay, 2016.
[28] OECD, Test No. 476: In Vitro Mammalian Cell Gene Mutation Tests using the Hprt and xprt genes, 2016.
[29] S.L. Smith-Roe, C.A. Hobbs, V. Hull, J.T. Auman, L. Recio, M.A. Streicker, M.V. Rivas, G.A. Pratt, F.Y. Lo, J.E. Higgins, E.K. Schmidt, L.N. Williams, D. Nachmanson, C.C. Valentine, 3rd, J.J. Salk, K.L. Witt, Adopting duplex sequencing™ technology for genetic toxicity testing: a proof-of-concept mutagenesis experiment with n-ethyl-n-nitrosourea (ENU)-exposed rats, bioRxiv (2023).
[30] E. Gocke, H. Bürgin, L. Müller, T. Pfister, Literature review on the genotoxicity, reproductive toxicity, and carcinogenicity of ethyl methanesulfonate, Toxicol. Lett. 190 (2009) 254–265.
[31] S.H. Doak, G.J. Jenkins, G.E. Johnson, E. Quick, E.M. Parry, J.M. Parry, Mechanistic influences for mutation induction curves after exposure to DNA-reactive carcinogens, Cancer Res 67 (2007) 3904–3911.

[32] R. Hoyos-Manchado, S. Villa-Consuegra, M. Berraquero, J. Jiménez, V.A. Tallada, Mutational analysis of N-ethyl-N-nitrosourea (ENU) in the fission yeast *Schizosaccharomyces pombe*, G3 (Bethesda) 10 (2020) 917–923.
[33] R. Benigni, C. Bossa, Mechanisms of chemical carcinogenicity and mutagenicity: a review with implications for predictive toxicology, Chem. Rev. 111 (2011) 2507–2536.
[34] T. Suzuki, M. Hayashi, X. Wang, K. Yamamoto, T. Ono, B.C. Myhr, T. Sofuni, A comparison of the genotoxicity of ethylnitrosourea and ethyl methanesulfonate in lacZ transgenic mice (Muta™Mouse), Mutat. Res 395 (1997) 75–82.
[35] J.A. Bueren-Calabuig, A. Negri, A. Morreale, F. Gago, Rationale for the opposite stereochemistry of the major monoadducts and interstrand crosslinks formed by mitomycin C and its decarbamoylated analogue at CpG steps in DNA and the effect of cytosine modification on reactivity, Org. Biomol. Chem. 10 (2012) 1543–1552.
[36] A. Takeiri, M. Mishima, K. Tanaka, A. Shioda, O. Ueda, H. Suzuki, M. Inoue, K. Masumura, T. Nohmi, Molecular characterization of mitomycin C-induced large deletions and tandem-base substitutions in the bone marrow of gpt delta transgenic mice, Chem. Res Toxicol. 16 (2003) 171–179.
[37] A. Takeiri, M. Mishima, K. Tanaka, A. Shioda, A. Harada, K. Watanabe, K. Masumura, T. Nohmi, A newly established GDL1 cell line from gpt delta mice well reflects the in vivo mutation spectra induced by mitomycin C, Mutat. Res 609 (2006) 102–115.
[38] V.N. Iyer, W. Szybalski, Mmitomycins and porfiromycin: chemical mechanism of activation and cross-linking of DNA, Science 145 (1964) 55–58.
[39] M.A. Beal, M.J. Meier, A. Dykes, C.L. Yauk, I.B. Lambert, F. Marchetti, The functional mutational landscape of the lacZ gene, iScience 26 (2023) 108407.
[40] K.S. Tao, C. Urlando, J.A. Heddle, Comparison of somatic mutation in a transgenic versus host locus, PNAS USA 90 (1993) 10681–10685.
[41] U.S. EPA, RIS Toxicological Review of Benzo[A]Pyrene (Final Report), U.S. Environmental Protection Agency, Washington, DC, 2017, pp. 1–234.
[42] A.L. Piberger, C.T. Krüger, B.M. Strauch, B. Schneider, A. Hartwig, BPDE-induced genotoxicity: relationship between DNA adducts, mutagenicity in the in vitro PIG-A assay, and the transcriptional response to DNA damage in TK6 cells, Arch. Toxicol. 92 (2018) 541–551.
[43] T. Souza, D. Jennen, J. van Delft, M. van Herwijnen, S. Kyrtoupolos, J. Kleinjans, New insights into BaP-induced toxicity: role of major metabolites in transcriptomics and contribution to hepatocarcinogenesis, Arch. Toxicol. 90 (2016) 1449–1458.
[44] A. Hakura, Y. Tsutsui, J. Sonoda, J. Kai, T. Imade, M. Shimada, Y. Sugihara, T. Mikami, Comparison between in vivo mutagenicity and carcinogenicity in multiple organs by benzo[a]pyrene in the lacZ transgenic mouse (Muta™Mouse), Mutat. Res 398 (1998) 123–130.
[45] C.C. Valentine, 3rd, R.R. Young, M.R. Fielden, R. Kulkarni, L.N. Williams, T. Li, S. Minocherhomji, J.J. Salk, Direct quantification of in vivo mutagenesis and carcinogenesis using duplex sequencing, PNAS USA 117 (2020) 33414–33425.
[46] IARC, Pharmaceuticals, a Review of Human Carcinogens, IARC Monographs on the Evaluation of Carcinogenic Risks to Humans, World Health Organization, 2012, pp. 319–329.
[47] C.C. Smith, G.E. Archer, E.J. Forster, T.R. Lambert, R.W. Rees, A.M. Lynch, Analysis of gene mutations and clastogenicity following short-term treatment with azathioprine in MutaMouse, Environ. Mol. Mutagen 34 (1999) 131–139.
[48] B.N. Cronstein, Pharmacogenetics in the rheumatic diseases, Ann. Rheum. Dis. 63 (2) (2004) ii25–ii27.
[49] F. Zhang, L. Fu, Y. Wang, 6-Thioguanine induces mitochondrial dysfunction and oxidative DNA damage in acute lymphoblastic leukemia cells, Mol. Cell Proteom. 12 (2013) 3803–3811.
[50] P. Karran, Thiopurines, DNA damage, DNA repair and therapy-related cancer, Br. Med Bull. 79-80 (2006) 153–170.
[51] P. Kasper, K. Tegethoff, L. Mueller, In vitro mutagenicity studies on cyproterone acetate using female rat hepatocytes for metabolic activation and as indicator cells, Carcinogenesis 16 (1995) 2309–2314.
[52] S. Werner, S. Kunz, T. Beckurts, C.D. Heidecke, T. Wolff, L.R. Schwarz, Formation of DNA adducts by cyproterone acetate and some structural analogues in primary cultures of human hepatocytes, Mutat. Res 395 (1997) 179–187.
[53] O. Krebs, B. Schafer, T. Wolff, D. Oesterle, E. Deml, M. Sund, J. Favor, The DNA damaging drug cyproterone acetate causes gene mutations and induces glutathione-S-transferase P in the liver of female Big Blue transgenic F344 rats, Carcinogenesis 19 (1998) 241–245.
[54] D. Kirkland, P. Kasper, H.J. Martus, L. Müller, J. van Benthem, F. Madia, R. Corvi, Updated recommended lists of genotoxic and non-genotoxic chemicals for assessment of the performance of new or improved genotoxicity tests, Mutat. Res 795 (2016) 7–30.